An Introduction to the Classical Three-Body Problem

From Periodic Solutions to Instabilities and Chaos

Govind S Krishnaswami and Himalaya Senapati

The classical three-body problem arose in an attempt to understand the effect of the Sun on the Moon's Keplerian orbit around the Earth. It has attracted the attention of some of the best physicists and mathematicians and led to the discovery of 'chaos'. We survey the three-body problem in its historical context and use it to introduce several ideas and techniques that have been developed to understand classical mechanical systems.

(Left) Govind Krishnaswami is on the faculty of the Chennai Mathematical Institute. His research concerns various problems in theoretical and mathematical physics.

(Right) Himalaya Senapati is a PhD student at the Chennai Mathematical Institute. He works on dynamical systems and chaos.

Keywords
Kepler problem, three-body problem, celestial mechanics, classical dynamics, chaos, instabilities.

1. Introduction

The three-body problem is one of the oldest problems in classical dynamics that continues to throw up surprises. It has challenged scientists from Newton's time to the present. It arose in an attempt to understand the Sun's effect on the motion of the Moon around the Earth. This was of much practical importance in marine navigation, where lunar tables were necessary to accurately determine longitude at sea (see *Box* 1).

The study of the three-body problem led to the discovery of the planet Neptune (see *Box* 2), it explains the location and stability of the Trojan asteroids and has furthered our understanding of the stability of the solar system [1]. Quantum mechanical variants of the three-body problem are relevant to the helium atom and water molecule [2].

The three-body problem admits many 'regular' solutions such as the collinear and equilateral periodic solutions of Euler and Lagrange as well as the more recently discovered figure-8 solution. On the other hand, it can also display chaos as serendipitously discovered by Poincaré. Though a general solution in closed form

> Euler had gone blind when he developed much of his lunar theory!

 https://doi.org/10.1007/s12045-019-0760-1

is not known, Sundman while studying binary collisions, discovered an exceptionally slowly converging series representation of solutions in fractional powers of time.

The three-body problem provides a context in which to study the development of classical dynamics as well as a window into several areas of mathematics (geometry, calculus and dynamical systems).

The importance of the three-body problem goes beyond its application to the motion of celestial bodies. As we will see, attempts to understand its dynamics have led to the discovery of many phenomena (e.g., the abundance of periodic motions, resonances (see *Box* 3), homoclinic points, collisional and non-collisional singularities, chaos and KAM tori) and techniques (e.g., Fourier series, perturbation theory, canonical transformations and regularization of singularities) with applications across the sciences.

Box 1. Longitude Act

The Longitude Act (1714) of the British Parliament offered £20,000 for a method to determine the longitude at sea to an accuracy of half a degree. This was important for marine navigation at a time of exploration of the continents. In the absence of accurate clocks that could function at sea, a lunar table along with the observed position of the Moon was the principal method of estimating the longitude. Leonhard Euler, Alexis Clairaut and Jean-Baptiste d'Alembert competed to develop a theory accounting for solar perturbations to the motion of the Moon around the Earth. For a delightful account of this chapter in the history of the three-body problem, including Clairaut's explanation of the annual 40° rotation of the lunar perigee (which had eluded Newton), see [3]. Interestingly, Clairaut's use of Fourier series in the three-body problem (1754) predates their use by Joseph Fourier in the analysis of heat conduction!

Box 2. Discovery of Neptune

The French mathematical astronomer Urbain Le Verrier (1846) was intrigued by the discrepancies between the observed and Keplerian orbits of Mercury and Uranus. He predicted the existence of Neptune (as was widely suspected) and calculated its expected position based on its effects on the motion of Uranus around the Sun (the existence and location of Neptune was independently inferred by John Adams in Britain). The German astronomer Johann Galle (working with his graduate student Heinrich d'Arrest) discovered Neptune within a degree of Le Verrier's predicted position on the very night that he received the latter's letter. It turned out that both Adams' and Le Verrier's heroic calculations were based on incorrect assumptions about Neptune, they were extremely lucky to stumble upon the correct location!

Box 3. Orbital Resonances

The simplest example of an orbital resonance occurs when the periods of two orbiting bodies (e.g., Jupiter and Saturn around the Sun) are in a ratio of small whole numbers ($T_S/T_J \approx 5/2$). Resonances can enhance their gravitational interaction and have both stabilizing and destabilizing effects. For instance, the moons Ganymede, Europa and Io are in a stable $1:2:4$ orbital resonance around Jupiter. The Kirkwood gaps in the asteroid belt are probably due to the destabilizing resonances with Jupiter. Resonances among the natural frequencies of a system (e.g., Keplerian orbits of a pair of moons of a planet) often lead to difficulties in naive estimates of the effect of a perturbation (say of the moons on each other).

2. Review of the Kepler Problem

As preparation for the three-body problem, we begin by reviewing some key features of the two-body problem.

If we ignore the non-zero size of celestial bodies, Newton's second law for the motion of two gravitating masses states that

$$m_1\ddot{\mathbf{r}}_1 = \alpha\frac{(\mathbf{r}_2-\mathbf{r}_1)}{|\mathbf{r}_1-\mathbf{r}_2|^3} \quad \text{and} \quad m_2\ddot{\mathbf{r}}_2 = \alpha\frac{(\mathbf{r}_1-\mathbf{r}_2)}{|\mathbf{r}_1-\mathbf{r}_2|^3}. \tag{1}$$

Here, $\alpha = Gm_1m_2$ measures the strength of the gravitational attraction and 'dots' denote time derivatives. This system has six degrees of freedom, say the three Cartesian coordinates of each mass $\mathbf{r}_1 = (x_1, y_1, z_1)$ and $\mathbf{r}_2 = (x_2, y_2, z_2)$. Thus, we have a system of 6 nonlinear (due to division by $|\mathbf{r}_1 - \mathbf{r}_2|^3$), second-order ordinary differential equations (ODEs) for the positions of the two masses. It is convenient to switch from $\mathbf{r}_1$ and $\mathbf{r}_2$ to the center of mass (CM) and relative coordinates

An advantage of the CM and relative coordinates is that in the absence of external forces, the CM moves at constant velocity, which can be chosen to vanish by going to a frame moving with the CM.

$$\mathbf{R} = \frac{m_1\mathbf{r}_1 + m_2\mathbf{r}_2}{m_1+m_2} \quad \text{and} \quad \mathbf{r} = \mathbf{r}_2 - \mathbf{r}_1. \tag{2}$$

In terms of these, the equations of motion (EOM) become

$$M\ddot{\mathbf{R}} = 0 \quad \text{and} \quad m\ddot{\mathbf{r}} = -\alpha\mathbf{r}/|\mathbf{r}|^3. \tag{3}$$

Here, $M = m_1 + m_2$ is the total mass and $m = m_1m_2/M$ the 'reduced' mass. The motion of the relative coordinate $\mathbf{r}$ decouples from that of $\mathbf{R}$ and describes a system with three degrees of freedom $\mathbf{r} = (x, y, z)$. Expressing the conservative gravitational force in terms of the gravitational potential $V = -\alpha/|\mathbf{r}|$, the equation

for the relative coordinate $\mathbf{r}$ becomes

$$\dot{\mathbf{p}} \equiv m\ddot{\mathbf{r}} = -\nabla_{\mathbf{r}} V = -\left(\frac{\partial V}{\partial x}, \frac{\partial V}{\partial y}, \frac{\partial V}{\partial z}\right), \tag{4}$$

where $\mathbf{p} = m\dot{\mathbf{r}}$ is the relative momentum. Taking the dot product with the 'integrating factor' $\dot{\mathbf{r}} = (\dot{x}, \dot{y}, \dot{z})$, we get

$$m\dot{\mathbf{r}} \cdot \ddot{\mathbf{r}} = \frac{d}{dt}\left(\frac{1}{2}m\dot{\mathbf{r}}^2\right) = -\left(\frac{\partial V}{\partial x}\,\dot{x} + \frac{\partial V}{\partial y}\,\dot{y} + \frac{\partial V}{\partial z}\,\dot{z}\right) = -\frac{dV}{dt}, \tag{5}$$

which implies that the energy $E \equiv \frac{1}{2}m\dot{\mathbf{r}}^2 + V$ or Hamiltonian $\frac{\mathbf{p}^2}{2m} + V$ is conserved. The relative angular momentum $\mathbf{L} = \mathbf{r} \times m\dot{\mathbf{r}} = \mathbf{r} \times \mathbf{p}$ is another constant of motion as the force is central : $\dot{\mathbf{L}} = \dot{\mathbf{r}} \times \mathbf{p} + \mathbf{r} \times \dot{\mathbf{p}} = 0 + 0$. The constancy of the direction of $\mathbf{L}$ implies planar motion in the CM frame: $\mathbf{r}$ and $\mathbf{p}$ always lie in the 'ecliptic plane' perpendicular to $\mathbf{L}$, which we take to be the x-y plane with origin at the CM (see *Figure* 1). The Kepler problem is most easily analyzed in plane-polar coordinates $\mathbf{r} = (r, \theta)$ in which the energy $E = \frac{1}{2}m\dot{r}^2 + V_{\text{eff}}(r)$ is the sum of a radial kinetic energy and an effective potential energy $V_{\text{eff}} = L_z^2/(2mr^2) + V(r)$. Here, $L_z = mr^2\dot{\theta}$ is the vertical component of angular momentum and the first term in V_{eff} is the centrifugal 'angular momentum barrier'. Since $\mathbf{L}$ (and therefore L_z) is conserved, V_{eff} depends only on r. Thus, θ does not appear in the Hamiltonian: it is a 'cyclic' coordinate. Conservation of energy constrains r to lie between 'turning points', i.e., zeros of $E - V_{\text{eff}}(r)$ where the radial velocity $\dot{r}$ momentarily vanishes. One finds that the orbits are Keplerian ellipses for $E < 0$ along with parabolae and hyperbolae for $E \geq 0$: $r(\theta) = \rho(1 + \epsilon\cos\theta)^{-1}$ [4, 5]. Here, $\rho = L_z^2/m\alpha$ is the radius of the circular orbit corresponding to angular momentum L_z, ϵ the eccentricity and $E = -\frac{\alpha}{2\rho}(1 - \epsilon^2)$ the energy.

The conservation of angular momentum in a central force is a consequence of rotation invariance: $V = V(|\mathbf{r}|)$ is independent of polar and azimuthal angles. More generally, Noether's theorem relates continuous symmetries to conserved quantities.

In addition to E and $\mathbf{L}$, the Laplace–Runge–Lenz (LRL) vector $\mathbf{A} = \mathbf{p} \times \mathbf{L} - m\alpha\,\hat{r}$ is another constant of motion. Thus, we have 7 conserved quantities: energy and three components each of $\mathbf{L}$ and $\mathbf{A}$. However, a system with three degrees of freedom has a six-dimensional phase space (space of coordinates and momenta, also called the state space) and if it is to admit continuous time evolution, it cannot have more than 5 independent conserved quantities.

The LRL vector $\mathbf{A}$ points along the semi-major axis from the CM to the perihelion and its magnitude determines the eccentricity of the orbit.

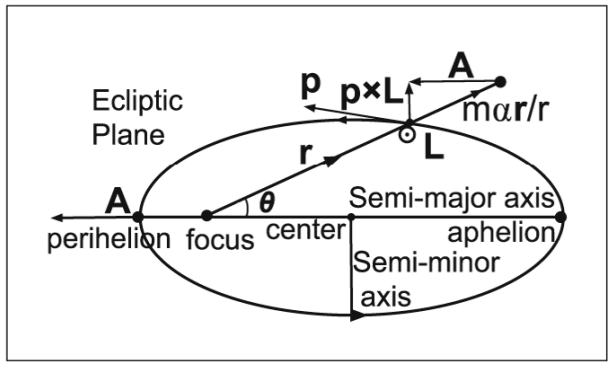

Figure 1. Keplerian ellipse in the ecliptic plane of motion showing the constant LRL vector **A**. The constant angular momentum **L** points out of the ecliptic plane.

The apparent paradox is resolved once we notice that E, $\mathbf{L}$ and $\mathbf{A}$ are not all independent; they satisfy two relations:

$$\mathbf{L} \cdot \mathbf{A} = 0 \quad \text{and} \quad E = \frac{\mathbf{A}^2 - m^2\alpha^2}{2m\mathbf{L}^2}. \tag{6}$$

Newton used the solution of the two-body problem to understand the orbits of planets and comets. He then turned his attention to the motion of the Moon around the Earth. Lunar motion is significantly affected by the Sun. For instance, $\mathbf{A}$ is *not* conserved and the lunar perigee rotates by 40° per year. Thus, he was led to study the Moon–Earth–Sun three-body problem.

Wolfgang Pauli (1926) derived the quantum mechanical spectrum of the Hydrogen atom using the relation between $E, \mathbf{L}^2$ and $\mathbf{A}^2$ before the development of the Schrödinger equation. Indeed, if we postulate circular Bohr orbits which have zero eccentricity ($\mathbf{A} = 0$) and quantized angular momentum $\mathbf{L}^2 = n^2\hbar^2$, then $E_n = -\frac{m\alpha^2}{2\hbar^2 n^2}$ where $\alpha = e^2/4\pi\epsilon_0$ is the electromagnetic analogue of Gm_1m_2.

3. The Three-Body Problem

We consider the problem of three point masses (m_a with position vectors $\mathbf{r}_a$ for $a = 1, 2, 3$) moving under their mutual gravitational attraction. This system has 9 degrees of freedom, whose dynamics is determined by 9 coupled second order nonlinear ODEs:

$$m_a \frac{d^2\mathbf{r}_a}{dt^2} = \sum_{b\neq a} Gm_a m_b \frac{\mathbf{r}_b - \mathbf{r}_a}{|\mathbf{r}_b - \mathbf{r}_a|^3} \quad \text{for} \quad a = 1, 2 \text{ and } 3. \tag{7}$$

As before, the three components of momentum $\mathbf{P} = \sum_a m_a\dot{\mathbf{r}}_a$, three components of angular momentum $\mathbf{L} = \sum_a \mathbf{r}_a \times \mathbf{p}_a$ and energy

$$E = \frac{1}{2}\sum_{a=1}^{3} m_a\dot{\mathbf{r}}_a^2 - \sum_{a<b} \frac{Gm_a m_b}{|\mathbf{r}_a - \mathbf{r}_b|} \equiv T + V, \tag{8}$$

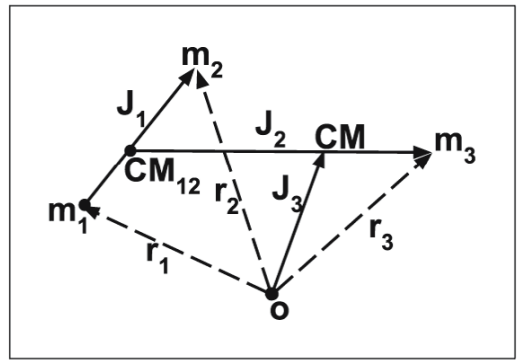

Figure 2. Jacobi vectors $\mathbf{J}_1, \mathbf{J}_2$ and $\mathbf{J}_3$ for the three-body problem. **O** is the origin of the coordinate system while CM_{12} is the center of mass of particles 1 and 2.

furnish 7 independent conserved quantities. Lagrange used these conserved quantities to reduce the above EOM to 7 first order ODEs (see *Box* 4).

Box 4. Lagrange's Reduction From 18 to 7 Equations

The 18 phase space variables of the three-body problem (components of $\mathbf{r}_1, \mathbf{r}_2, \mathbf{r}_3, \mathbf{p}_1, \mathbf{p}_2, \mathbf{p}_3$) satisfy 18 first order ODEs $\dot{\mathbf{r}}_a = \mathbf{p}_a$, $\dot{\mathbf{p}}_a = -\nabla_{\mathbf{r}_a} V$. Lagrange (1772) used the conservation laws to reduce these ODEs to a system of 7 first order ODEs. Conservation of momentum determines 6 phase space variables comprising the location $\mathbf{R}_{\rm CM}$ and momentum $\mathbf{P}$ of the CM. Conservation of angular momentum $\mathbf{L} = \sum \mathbf{r}_a \times \mathbf{p}_a$ and energy E lead to 4 additional constraints. By using one of the coordinates as a parameter along the orbit (in place of time), Lagrange reduced the three-body problem to a system of 7 first order nonlinear ODEs.

Jacobi vectors (see *Figure* 2) generalize the notion of CM and relative coordinates to the three-body problem [6]. They are defined as $\mathbf{J}_1 = \mathbf{r}_2 - \mathbf{r}_1$,

$$\mathbf{J}_2 = \mathbf{r}_3 - \frac{m_1\mathbf{r}_1 + m_2\mathbf{r}_2}{m_1 + m_2} \quad \text{and} \quad \mathbf{J}_3 = \frac{m_1\mathbf{r}_1 + m_2\mathbf{r}_2 + m_3\mathbf{r}_3}{m_1 + m_2 + m_3}. \qquad (9)$$

$\mathbf{J}_3$ is the coordinate of the CM, $\mathbf{J}_1$ the position vector of m_2 relative to m_1 and $\mathbf{J}_2$ that of m_3 relative to the CM of m_1 and m_2. A nice feature of Jacobi vectors is that the kinetic energy $T = \frac{1}{2}\sum_{a=1,2,3} m_a\dot{\mathbf{r}}_a^2$ and moment of inertia $I = \sum_{a=1,2,3} m_a\mathbf{r}_a^2$, regarded as quadratic forms, remain diagonal:

$$T = \frac{1}{2}\sum_{1\le a\le 3} M_a\dot{\mathbf{J}}_a^2 \quad \text{and} \quad I = \sum_{1\le a\le 3} M_a\mathbf{J}_a^2. \qquad (10)$$

A quadratic form $\sum_{a,b} r_a Q_{ab} r_b$ is diagonal if $Q_{ab} = 0$ for $a \neq b$. Here, $M_1^{-1} = m_1^{-1} + m_2^{-1}$ is the reduced mass of the first pair, $M_2^{-1} = (m_1 + m_2)^{-1} + m_3^{-1}$ is the reduced mass of m_3 and the (m_1, m_2) system and $M_3 = m_1 + m_2 + m_3$ the total mass.

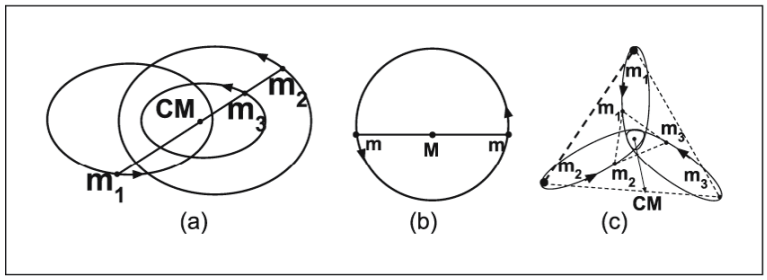

Figure 3. (**a, b**) Euler collinear periodic solutions with three masses traversing Keplerian ellipses/circles with one focus at the CM. The constant ratios of separations are functions of the mass ratios alone. **(c)** Lagrange's periodic solution with three bodies at vertices of equilateral triangles.

Moreover, just as the potential energy $-\alpha/|\mathbf{r}|$ in the 2-body problem is a function only of the relative coordinate $\mathbf{r}$, here the potential energy V may be expressed entirely in terms of $\mathbf{J}_1$ and $\mathbf{J}_2$:

$$V = -\frac{Gm_1m_2}{|\mathbf{J}_1|} - \frac{Gm_2m_3}{|\mathbf{J}_2 - \mu_1\mathbf{J}_1|} - \frac{Gm_3m_1}{|\mathbf{J}_2 + \mu_2\mathbf{J}_1|} \quad \text{where} \quad \mu_{1,2} = \frac{m_{1,2}}{m_1 + m_2}. \tag{11}$$

Thus, the components of the CM vector $\mathbf{J}_3$ are cyclic coordinates in the Hamiltonian $H = T + V$. In other words, the center of mass motion ($\ddot{\mathbf{J}}_3 = 0$) decouples from that of $\mathbf{J}_1$ and $\mathbf{J}_2$.

An instantaneous configuration of the three bodies defines a triangle with masses at its vertices. The moment of inertia about the center of mass $I_{\rm CM} = M_1\mathbf{J}_1^2 + M_2\mathbf{J}_2^2$ determines the size of the triangle. For instance, particles suffer a triple collision when $I_{\rm CM} \to 0$ while $I_{\rm CM} \to \infty$ when one of the bodies flies off to infinity.

4. Euler and Lagrange Periodic Solutions

The planar three-body problem is the special case where the masses always lie on a fixed plane. For instance, this happens when the CM is at rest ($\dot{\mathbf{J}}_3 = 0$) and the angular momentum about the CM vanishes ($\mathbf{L}_{\rm CM} = M_1\mathbf{J}_1 \times \dot{\mathbf{J}}_1 + M_2\mathbf{J}_2 \times \dot{\mathbf{J}}_2 = 0$). In 1767, the Swiss scientist Leonhard Euler discovered simple periodic solutions to the planar three-body problem where the masses are always collinear, with each body traversing a Keplerian orbit about their common CM. The line through the masses rotates about the CM with the ratio of separations remaining constant (see *Figure* 3). The Italian/French mathematician Joseph-Louis Lagrange rediscovered Euler's solution in 1772 and also found new periodic

In Lagrange's solutions, bodies lie at vertices of equilateral triangles while they are collinear in Euler's solutions. In both cases, the force on each body is always toward the common center of mass and proportional to the distance from it.

solutions where the masses are always at the vertices of equilateral triangles (see *Figure* 3c).

In Lagrange's equilateral solution, the size and angular orientation of the triangle may change with time. In the limiting case of zero angular momentum, the three bodies move toward or away from their CM along straight lines. These implosion or explosion solutions are called Lagrange homotheties.

It is convenient to identify the plane of motion with the complex plane $\mathbb{C}$ and let the three complex numbers $z_{a=1,2,3}(t)$ denote the positions of the three masses at time t. For e.g., the real and imaginary parts of z_1 denote the Cartesian components of the position vector $\mathbf{r}_1$ of the first mass. In Lagrange's solutions, $z_a(t)$ lie at the vertices of an equilateral triangle while they are collinear in Euler's solutions. In both cases, the force on each body is always toward the common CM and proportional to the distance from it. For instance, the force on m_1 in a Lagrange solution is:

$$\begin{aligned}\mathbf{F}_1 &= Gm_1m_2\frac{\mathbf{r}_2-\mathbf{r}_1}{|\mathbf{r}_2-\mathbf{r}_1|^3}+Gm_1m_3\frac{\mathbf{r}_3-\mathbf{r}_1}{|\mathbf{r}_3-\mathbf{r}_1|^3}\\ &= \frac{Gm_1}{d^3}\left(m_1\mathbf{r}_1+m_2\mathbf{r}_2+m_3\mathbf{r}_3-M_3\mathbf{r}_1\right), \qquad (12)\end{aligned}$$

where $d = |\mathbf{r}_2 - \mathbf{r}_1| = |\mathbf{r}_3 - \mathbf{r}_1|$ is the side-length of the equilateral triangle and $M_3 = m_1 + m_2 + m_3$. Recalling that $\mathbf{r}_{\rm CM} = (m_1\mathbf{r}_1 + m_2\mathbf{r}_2 + m_3\mathbf{r}_3)/M_3$, we get

$$\mathbf{F}_1 = \frac{Gm_1}{d^3}M_3\left(\mathbf{r}_{\rm CM}-\mathbf{r}_1\right) \equiv Gm_1\delta_1\frac{\mathbf{r}_{\rm CM}-\mathbf{r}_1}{|\mathbf{r}_{\rm CM}-\mathbf{r}_1|^3}, \qquad (13)$$

where $\delta_1 = M_3|\mathbf{r}_{\rm CM} - \mathbf{r}_1|^3/d^3$ is a function of the masses alone[1]. Thus, the equation of motion for m_1,

$$m_1\ddot{\mathbf{r}}_1 = Gm_1\delta_1(\mathbf{r}_{\rm CM}-\mathbf{r}_1)/(|\mathbf{r}_{\rm CM}-\mathbf{r}_1|^3), \qquad (14)$$

takes the same form as in the two-body Kepler problem [see (1)]. The same applies to m_2 and m_3. So if $z_a(0)$ denote the initial positions, the curves $z_a(t) = z(t)z_a(0)$ are solutions of Newton's equations for three bodies provided $z(t)$ is a Keplerian orbit for an appropriate two-body problem. In other words, each mass traverses a rescaled Keplerian orbit about the common centre of mass. A similar analysis applies to the Euler collinear solutions as well: locations of the masses is determined by the requirement that the force on each one is toward the CM and proportional to the distance from it (see *Box* 5 on central configurations).

[1] Indeed, $M_3(\mathbf{r}_{\rm CM} - \mathbf{r}_1) = m_2(\mathbf{r}_2 - \mathbf{r}_1) + m_3(\mathbf{r}_3 - \mathbf{r}_1) \equiv m_2\mathbf{b} + m_3\mathbf{c}$ where $\mathbf{b}$ and $\mathbf{c}$ are two of the sides of the equilateral triangle of length d. This leads to $|(\mathbf{r}_{\rm CM} - \mathbf{r}_1)/d| = (1/M_3)\sqrt{m_2^2 + m_3^2 + m_2m_3}$ which is a function of masses alone.

Box 5. Central Configurations

Three-body configurations in which the acceleration of each particle points towards the CM and is proportional to its distance from the CM ($\mathbf{a}_b = \omega^2(\mathbf{R}_{\rm CM} - \mathbf{r}_b)$ for $b = 1, 2, 3$) are called 'central configurations'. A central configuration rotating at angular speed ω about the CM automatically satisfies the equations of motion (7). Euler collinear and Lagrange equilateral configurations are the only central configurations in the three-body problem. In 1912, Karl Sundmann showed that triple collisions are asymptotically central configurations.

5. Restricted Three-Body Problem

The restricted three-body problem is a simplified version of the three-body problem where one of the masses m_3 is assumed much smaller than the primaries m_1 and m_2. Thus, m_1 and m_2 move in Keplerian orbits which are not affected by m_3. In the planar circular restricted three-body problem, the primaries move in fixed circular orbits around their common CM with angular speed $\Omega = (G(m_1+m_2)/d^3)^{1/2}$ given by Kepler's third law and m_3 moves in the same plane as m_1 and m_2. Here, d is the separation between the primaries. This system has 2 degrees of freedom associated to the planar motion of m_3, and therefore, a 4-dimensional phase space just like the planar Kepler problem for the reduced mass. However, unlike the latter which has three conserved quantities (energy, z-component of angular momentum and direction of LRL vector) and is exactly solvable, the planar restricted three-body problem has only one known conserved quantity, the 'Jacobi integral', which is the energy of m_3 in the co-rotating (non-inertial) frame of the primaries:

The Sun–Earth–Moon system provides an example of the restricted three-body problem where we further have $m_2 = m_{\rm E} \ll m_1 = m_{\rm S}$.

$$E = \left[\frac{1}{2}m_3\dot{r}^2 + \frac{1}{2}m_3 r^2\dot{\phi}^2\right] - \frac{1}{2}m_3\Omega^2 r^2 - Gm_3\left(\frac{m_1}{r_1} + \frac{m_2}{r_2}\right) \equiv T + V_{\rm eff}. \tag{15}$$

The 'Roche' effective potential $V_{\rm eff}$, named after the French astronomer Édouard Albert Roche, is a sum of centrifugal and gravitational energies due to m_1 and m_2.

Here, (r, ϕ) are the plane polar coordinates of m_3 in the co-rotating frame of the primaries with origin located at their CM while r_1 and r_2 are the distances of m_3 from m_1 and m_2 (see *Figure* 4).

A system with n degrees of freedom needs at least n constants of motion to be exactly solvable. For the restricted three-body

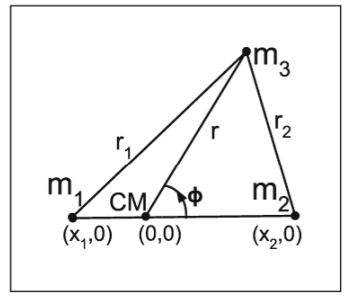

Figure 4. The secondary m_3 in the co-rotating frame of primaries m_1 and m_2 in the restricted three-body problem. The origin is located at the CM of m_1 and m_2 which coincides with the CM of the system since $m_3 \ll m_{1,2}$.

problem, Henri Poincaré (1889) proved the nonexistence of any conserved quantity (other than E) that is analytic in small mass ratios (m_3/m_2 and $(m_3+m_2)/m_1$) and orbital elements ($\mathbf{J}_1$, $M_1\dot{\mathbf{J}}_1$, $\mathbf{J}_2$ and $M_2\dot{\mathbf{J}}_2$) [7, 8, 9]. This was an extension of a result of Heinrich Bruns who had proved in 1887 the nonexistence of any new conserved quantity algebraic in Cartesian coordinates and momenta for the general three-body problem [10]. Thus, roughly speaking, Poincaré showed that the restricted three-body problem is not exactly solvable. In fact, as we outline in §7., he discovered that it displays chaotic behavior.

A Hamiltonian system with n degrees of freedom is exactly solvable in the sense of Liouville if it possesses n independent conserved quantities in involution, i.e., with vanishing pairwise Poisson brackets (see *Boxes* 6 and 10).

Euler and Lagrange points (denoted L_{1-5}) of the restricted three-body problem are the locations of a third mass ($m_3 \ll m_1, m_2$) in the co-rotating frame of the primaries m_1 and m_2 in the Euler and Lagrange solutions (see *Figure* 5). Their stability would allow an asteroid or satellite to occupy a Lagrange point. Euler points $L_{1,2,3}$ are saddle points of the Roche potential while $L_{4,5}$ are maxima (see *Figure* 6). This suggests that they are all unstable. However, V_{eff} does not include the effect of the Coriolis force since it does no work. A more careful analysis shows that the Coriolis force stabilises $L_{4,5}$. It is a bit like a magnetic force which does no work but can stabilise a particle in a Penning trap. Euler points are always unstable while the Lagrange points $L_{4,5}$ are stable to small perturbations iff $(m_1+m_2)^2 \geq 27m_1m_2$ [11]. More generally, in the unrestricted three-body problem, the Lagrange equilateral solutions are stable iff:

Lagrange points L_{1-5} are also called libration (literally, balance) points.

Stable 'Halo' orbits around Euler points have been found numerically.

$$(m_1+m_2+m_3)^2 \geq 27(m_1m_2+m_2m_3+m_3m_1). \qquad (16)$$

The above criterion due to Edward Routh (1877) is satisfied if

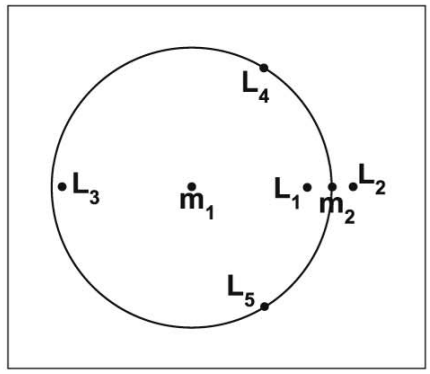

Figure 5. The positions of Euler ($L_{1,2,3}$) and Lagrange ($L_{4,5}$) points when $m_1 \gg m_2 \gg m_3$. m_2 is in an approximately circular orbit around m_1. L_3 is almost diametrically opposite to m_2 and a bit closer to m_1 than m_2 is. L_1 and L_2 are symmetrically located on either side of m_2. L_4 and L_5 are equidistant from m_1 and m_2 and lie on the circular orbit of m_2.

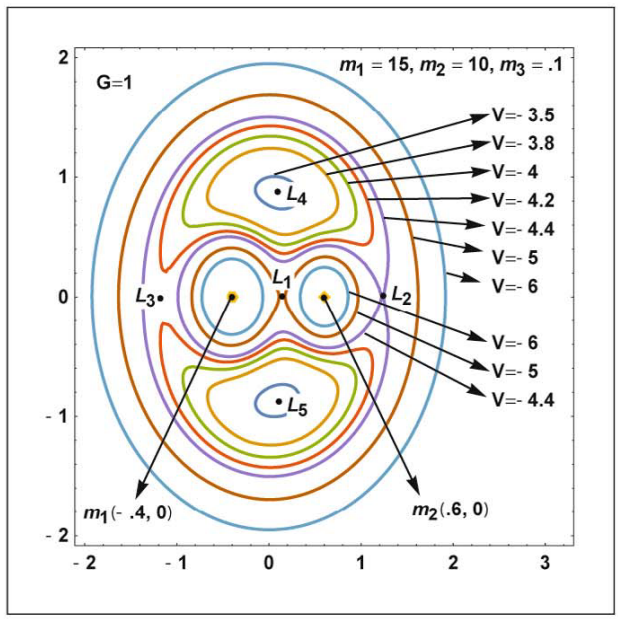

Figure 6. Level curves of the Roche effective potential energy V_{eff} of m_3 in the co-rotating frame of the primaries m_1 and m_2 in the circular restricted three-body problem for $G = 1$, $m_1 = 15, m_2 = 10$ and $m_3 = .1$. Lagrange points L_{1-5} are at extrema of V_{eff}. The trajectory of m_3 for a given energy E must lie in the Hill region defined by $V_{\text{eff}}(x, y) \leq E$. E.g., for $E = -6$, the Hill region is the union of two neighbourhoods of the primaries and a neighborhood of the point at infinity. The lobes of the ∞-shaped level curve passing through L_1 are called Roche's lobes. The saddle point L_1 is like a mountain pass through which material could pass between the lobes.

one of the masses dominates the other two. For instance, $L_{4,5}$ for the Sun–Jupiter system are stable and occupied by the Trojan asteroids.

6. Planar Euler Three-Body Problem

Given the complexity of the restricted three-body problem, Euler (1760) proposed the even simpler problem of a mass m moving in

Unlike in the restricted three-body problem, in the Euler three-body, the rest-frame of the primaries is an inertial frame, so there are no centrifugal or Coriolis forces. This simplification allows the Euler three-body problem to be exactly solved.

the gravitational potential of two *fixed* masses m_1 and m_2. Initial conditions can be chosen so that m always moves on a fixed plane containing m_1 and m_2. Thus, we arrive at a one-body problem with two degrees of freedom and energy:

$$E = \frac{1}{2}m\left(\dot{x}^2 + \dot{y}^2\right) - \frac{\mu_1}{r_1} - \frac{\mu_2}{r_2}. \tag{17}$$

Here, (x, y) are the Cartesian coordinates of m, r_a the distances of m from m_a and $\mu_a = Gm_a m$ for $a = 1, 2$ (see *Figure* 7).

Just as the Kepler problem simplifies in plane-polar coordinates (r, θ) centered at the CM, the Euler three-body problem simplifies in an elliptical coordinate system (ξ, η). The level curves of ξ and η are mutually orthogonal confocal ellipses and hyperbolae (see *Figure* 7) with the two fixed masses at the foci $2f$ apart:

$$x = f\ \cosh\xi\ \cos\eta \quad \text{and} \quad y = f\ \sinh\xi\ \sin\eta. \tag{18}$$

Here, ξ and η are like the radial distance r and angle θ, whose level curves are mutually orthogonal concentric circles and radial rays. The distances of m from $m_{1,2}$ are $r_{1,2} = f(\cosh\xi \mp \cos\eta)$.

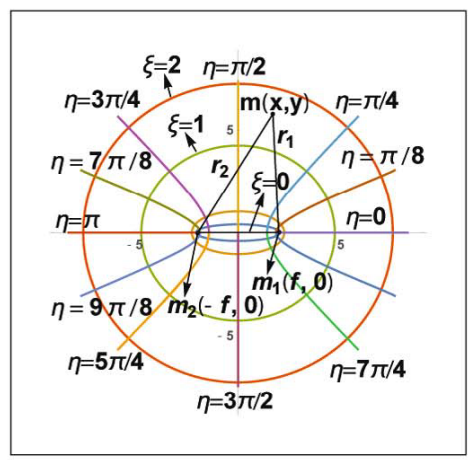

Figure 7. Elliptical coordinate system for the Euler three-body problem. Two masses are at the foci $(\pm f, 0)$ of an elliptical coordinate system with $f = 2$ on the x-y plane. The level curves of ξ and η (confocal ellipses and hyperbolae) are indicated.

Box 6. Canonical Transformations

We have seen that the Kepler problem is more easily solved in polar coordinates and momenta $(r, \theta, p_r, p_\theta)$ than in Cartesian phase space variables (x, y, p_x, p_y). This change is an example of a canonical transformation (CT). More generally, a CT is a change of canonical phase space variables $(\mathbf{q}, \mathbf{p}) \rightarrow (\mathbf{Q}(\mathbf{p}, \mathbf{q}, t), \mathbf{P}(\mathbf{p}, \mathbf{q}, t))$ that preserves the form of Hamilton's equations. For one degree of freedom, Hamilton's equations $\dot{q} = \frac{\partial H}{\partial p}$ and $\dot{p} = -\frac{\partial H}{\partial q}$ become $\dot{Q} = \frac{\partial K}{\partial P}$ and $\dot{P} = -\frac{\partial K}{\partial Q}$ where $K(Q, P, t)$ is the new Hamiltonian (for a time independent CT, the old and new Hamiltonians are related by substitution: $H(q, p) = K(Q(q, p), P(q, p))$). The form of Hamilton's equations is preserved provided the basic Poisson brackets (PB) do not change i.e.,

$$\{q, p\} = 1, \;\; \{q, q\} = \{p, p\} = 0 \quad \Rightarrow \quad \{Q, P\} = 1, \;\; \{Q, Q\} = \{P, P\} = 0. \tag{19}$$

Here, the Poisson bracket of two functions on phase space $f(q, p)$ and $g(q, p)$ is defined as

$$\{f(q, p), g(q, p)\} = \frac{\partial f}{\partial q}\frac{\partial g}{\partial p} - \frac{\partial f}{\partial p}\frac{\partial g}{\partial q}. \tag{20}$$

For one degree of freedom, a CT is simply an area and orientation preserving transformation of the q-p phase plane. Indeed, the condition $\{Q, P\} = 1$ simply states that the Jacobian determinant $J = \det\left(\frac{\partial Q}{\partial q}, \frac{\partial Q}{\partial p} \mid \frac{\partial P}{\partial q}, \frac{\partial P}{\partial p}\right) = 1$ so that the new area element $dQ\,dP = J\,dq\,dp$ is equal to the old one. A CT can be obtained from a suitable generating function, say of the form $S(q, P, t)$, in the sense that the equations of transformation are given by partial derivatives of S:

$$p = \frac{\partial S}{\partial q}, \quad Q = \frac{\partial S}{\partial P} \quad \text{and} \quad K = H + \frac{\partial S}{\partial t}. \tag{21}$$

For example, $S = qP$ generates the identity transformation ($Q = q$ and $P = p$) while $S = -qP$ generates a rotation of the phase plane by π ($Q = -q$ and $P = -p$).

The above confocal ellipses and hyperbolae are Keplerian orbits when a single fixed mass (m_1 or m_2) is present at one of the foci $(\pm f, 0)$. Remarkably, these Keplerian orbits survive as orbits of the Euler three-body problem. This is a consequence of Bonnet's theorem, which states that if a curve is a trajectory in two separate force fields, it remains a trajectory in the presence of both. If v_1 and v_2 are the speeds of the Keplerian trajectories when only m_1 or m_2 was present, then $v = \sqrt{v_1^2 + v_2^2}$ is the speed when both are present.

Box 7. Hamilton–Jacobi Equation

The Hamilton–Jacobi (HJ) equation is an alternative formulation of Newtonian dynamics. Let $i = 1, \ldots, n$ label the degrees of freedom of a mechanical system. Cyclic coordinates q^i (i.e., those that do not appear in the Hamiltonian $H(\mathbf{q}, \mathbf{p}, t)$ so that $\partial H/\partial q^i = 0$) help to understand Newtonian trajectories, since their conjugate momenta p_i are conserved ($\dot{p}_i = \frac{\partial H}{\partial q^i} = 0$). If all coordinates are cyclic, then each of them evolves linearly in time: $q^i(t) = q^i(0) + \frac{\partial H}{\partial p_i} t$. Now time-evolution is *even simpler* if $\frac{\partial H}{\partial p_i} = 0$ for all i as well, i.e., if H is independent of both coordinates and momenta! In the HJ approach, we find a CT from old phase space variables $(\mathbf{q}, \mathbf{p})$ to such a coordinate system $(\mathbf{Q}, \mathbf{P})$ in which the new Hamiltonian K is a constant (which can be taken to vanish by shifting the zero of energy). The HJ equation is a nonlinear, first-order partial differential equation (PDE) for Hamilton's principal function $S(\mathbf{q}, \mathbf{P}, t)$ which generates the canonical transformation from $(\mathbf{q}, \mathbf{p})$ to $(\mathbf{Q}, \mathbf{P})$. As explained in *Box* 6, this means $p_i = \frac{\partial S}{\partial q^i}$, $Q^j = \frac{\partial S}{\partial P_j}$ and $K = H + \frac{\partial S}{\partial t}$. Thus, the HJ equation

$$H\left(\mathbf{q}, \frac{\partial S}{\partial \mathbf{q}}, t\right) + \frac{\partial S}{\partial t} = 0 \tag{22}$$

is simply the condition for the new Hamiltonian K to vanish. If H is time-independent, we may 'separate' the time-dependence of S by writing $S(\mathbf{q}, \mathbf{P}, t) = W(\mathbf{q}, \mathbf{P}) - Et$ where the 'separation constant' E may be interpreted as energy. Thus, the time independent HJ-equation for Hamilton's characteristic function W is

$$H\left(\mathbf{q}, \frac{\partial W}{\partial \mathbf{q}}\right) = E. \tag{23}$$

E.g., for a particle in a potential $V(\mathbf{q})$, it is the equation $\frac{1}{2m}\left(\frac{\partial W}{\partial \mathbf{q}}\right)^2 + V(\mathbf{q}) = E$. By solving (23) for W, we find the desired canonical transformation to the new conserved coordinates $\mathbf{Q}$ and momenta $\mathbf{P}$. By inverting the relation $(q, p) \mapsto (Q, P)$ we find $(q^i(t), p_j(t))$ given their initial values. W is said to be a *complete integral* of the HJ equation if it depends on n constants of integration, which may be taken to be the new momenta $P_1, \ldots, P_n$. When this is the case, the system is said to be integrable via the HJ equation. However, it is seldom possible to find such a complete integral. In favourable cases, *separation of variables* can help to solve the HJ equation (see *Box* 8).

When the primaries coalesce at the origin ($f \to 0$), Whittaker's constant reduces to the conserved quantity $\mathbf{L}^2$ of the planar 2-body problem.

Bonnet's theorem however does not give us all the trajectories of the Euler three-body problem. More generally, we may integrate the equations of motion by the method of separation of variables in the Hamilton–Jacobi equation (see [12] and *Boxes* 6, 7 and 8). The system possesses *two* independent conserved quantities: energy and Whittaker's constant [2, 10]

$$\begin{aligned} w &= \mathbf{L}_1 \cdot \mathbf{L}_2 + 2mf\left(-\mu_1 \cos\theta_1 + \mu_2 \cos\theta_2\right) \\ &= m^2 r_1^2 r_2^2\, \dot{\theta}_1 \dot{\theta}_2 + 2fm\left(-\mu_1 \cos\theta_1 + \mu_2 \cos\theta_2\right). \end{aligned} \tag{24}$$

Here, θ_a are the angles between the position vectors $\mathbf{r}_a$ and the positive x-axis and $\mathbf{L}_{1,2} = mr_{1,2}^2\dot{\theta}_{1,2}\hat{z}$ are the angular momenta about the two force centers (*Figure* 7). Since w is conserved, it Poisson commutes with the Hamiltonian H. Thus, the planar Euler three-body problem has two degrees of freedom and two conserved quantities in involution. Consequently, the system is integrable in the sense of Liouville.

Box 8. Separation of Variables

In the planar Euler three-body problem, Hamilton's characteristic function W depends on the two 'old' elliptical coordinates ξ and η. The virtue of elliptical coordinates is that the time-independent HJ equation can be solved by separating the dependence of W on ξ and η: $W(\xi,\eta) = W_1(\xi) + W_2(\eta)$. Writing the energy (17) in elliptical coordinates (18) and using $p_\xi = W_1'(\xi)$ and $p_\eta = W_2'(\eta)$, the time-independent HJ equation (23) becomes

$$E = \frac{W_1'(\xi)^2 + W_2'(\eta)^2 - 2mf(\mu_1+\mu_2)\cosh\xi - 2mf(\mu_1-\mu_2)\cos\eta}{2mf^2(\cosh^2\xi - \cos^2\eta)}. \tag{25}$$

Rearranging,

$$W_1'^2 - 2Emf^2\cosh^2\xi - 2mf(\mu_1+\mu_2)\cosh\xi = -W_2'^2 - 2Emf^2\cos^2\eta + 2mf(\mu_1-\mu_2)\cos\eta. \tag{26}$$

Since the LHS and RHS are functions only of ξ and η respectively, they must both be equal to a 'separation constant' α. Thus, the HJ PDE separates into a pair of decoupled ODEs for $W_1(\xi)$ and $W_2(\eta)$. The latter may be integrated using elliptic functions. Note that Whittaker's constant w (24) may be expressed as $w = -2mf^2E - \alpha$.

More generally, in the three-dimensional Euler three-body problem, the mass m can revolve (non-uniformly) about the line joining the force centers (x-axis) so that its motion is no longer confined to a plane. Nevertheless, the problem is exactly solvable as the equations admit three independent constants of motion in involution: energy, Whittaker's constant and the x component of angular momentum [2].

7. Some Landmarks in the History of the Three-Body Problem

Developments that arose from attempts to solve the three-body problem have had an impact across the sciences.

The importance of the three-body problem lies in part in the developments that arose from attempts to solve it [7, 8]. These have had an impact all over astronomy, physics, and mathematics.

Can planets collide, be ejected from the solar system or suffer significant deviations from their Keplerian orbits? This is the question of the stability of the solar system. In the 18th century, Pierre-Simon Laplace and J L Lagrange obtained the first significant results on stability. They showed that to first order in the ratio of planetary to solar masses (M_p/M_S), there is no unbounded variation in the semi-major axes of the orbits, indicating stability of the solar system. Siméon Denis Poisson extended this result to second order in M_p/M_S. However, in what came as a surprise, the Romanian Spiru Haretu (1878) overcame significant technical challenges to find secular terms (growing linearly and quadratically in time) in the semi-major axes at third order! This was an example of a perturbative expansion, where one expands a physical quantity in powers of a small parameter (here the semi-major axis was expanded in powers of $M_p/M_S \ll 1$). Haretu's result however did not prove instability as the effects of his secular terms could cancel out (see *Box* 9 for a simple example). But it effectively put an end to the hope of proving the stability or instability of the solar system using such a perturbative approach.

Haretu's results essentially put an end to the hope of proving the stability or instability of the solar system using a perturbative approach.

The scale of Delaunay's hand calculations is staggering: he applied a succession of 505 canonical transformations to a 7^{th} order perturbative treatment of the three-dimensional elliptical restricted three-body problem.

The development of Hamilton's mechanics and its refinement in the hands of Carl Jacobi was still fresh when the French dynamical astronomer Charles Delaunay (1846) began the first extensive use of canonical transformations (see *Box* 6) in perturbation theory [13]. He arrived at the EOM for m_3 in Hamiltonian form using 3 pairs of canonically conjugate orbital variables (3 angular momentum components, the true anomaly, longitude of the ascending node and distance of the ascending node from perigee). He obtained the latitude and longitude of the Moon in trigonometric series of about 450 terms with secular terms eliminated (see *Box* 9). It wasn't till 1970–71 that Delaunay's heroic calcu-

lations were checked and extended using computers at the Boeing Scientific Laboratories [13]!

Box 9. Poincaré–Lindstedt Method

The Poincaré-Lindstedt method is an approach to finding series solutions to a system such as the anharmonic oscillator $\ddot{x} + x + gx^3 = 0$, which for small g, is a perturbation of the harmonic oscillator $m\ddot{x} + kx = 0$ with mass $m = 1$ and spring constant $k = 1$. The latter admits the periodic solution $x_0(t) = \cos t$ with initial conditions $x(0) = 1$, $\dot{x}(0) = 0$. For a small perturbation $0 < g \ll 1$, expanding $x(t) = x_0(t) + gx_1(t) + \cdots$ in powers of g leads to a linearized equation for $x_1(t)$

$$\ddot{x}_1 + x_1 + \cos^3 t = 0. \tag{27}$$

However, the perturbative solution

$$x(t) = x_0 + gx_1 + O(g^2) = \cos t + g\left[\frac{1}{32}(\cos 3t - \cos t) - \frac{3}{8}t\sin t\right] + O(g^2) \tag{28}$$

is unbounded due to the linearly growing *secular* term $(-3/8)t\sin t$. This is unacceptable as the energy $E = \frac{1}{2}\dot{x}^2 + \frac{1}{2}x^2 + \frac{1}{4}gx^4$ must be conserved and the particle must oscillate between turning points of the potential $V = \frac{1}{2}x^2 + \frac{g}{4}x^4$. The Poincaré–Lindstedt method avoids this problem by looking for a series solution of the form

$$x(t) = x_0(\tau) + g\tilde{x}_1(\tau) + \cdots, \tag{29}$$

where $\tau = \omega t$ with $\omega = 1 + g\omega_1 + \cdots$. The constants $\omega_1, \omega_2, \cdots$ are chosen to ensure that the coefficients of the secular terms at order $g, g^2, \cdots$ vanish. In the case at hand, we have

$$x(t) = \cos(t + g\omega_1 t) + g\tilde{x}_1(t) + O(g^2) = \cos t + g\tilde{\tilde{x}}_1(t) + O(g^2) \quad \text{where} \quad \tilde{\tilde{x}}_1(t) = \tilde{x}_1(t) - \omega_1 t\sin t. \tag{30}$$

$\tilde{\tilde{x}}_1$ satisfies the same equation (27) as x_1 did, leading to

$$\tilde{x}_1(t) = \frac{1}{32}(\cos 3t - \cos t) + \left(\omega_1 - \frac{3}{8}\right)t\sin t. \tag{31}$$

The choice $\omega_1 = 3/8$ ensures cancellation of the secular term at order g, leading to the approximate bounded solution

$$x(t) = \cos\left(t + \frac{3}{8}gt\right) + \frac{g}{32}(\cos 3t - \cos t) + O\left(g^2\right). \tag{32}$$

The Swede Anders Lindstedt (1883) developed a systematic method to approximate solutions to nonlinear ODEs when naive perturbation series fail due to secular terms (see *Box* 9). The technique

was further developed by Poincaré. Lindstedt assumed the series to be generally convergent, but Poincaré soon showed that they are divergent in most cases. Remarkably, nearly 70 years later, Kolmogorov, Arnold and Moser showed that in many of the cases where Poincaré's arguments were inconclusive, the series are in fact convergent, leading to the celebrated KAM theory of integrable systems subject to small perturbations (see *Box* 10).

Box 10. Action-Angle Variables and Invariant Tori

Time evolution is particularly simple if all the generalized coordinates θ^j are cyclic so that their conjugate momenta I_j are conserved: $\dot{I}_j = -\frac{\partial H}{\partial \theta^j} = 0$. A Hamiltonian system with n degrees of freedom is integrable in the sense of Liouville if it admits n canonically conjugate ($\{\theta^j, I_k\} = \delta^j_k$) pairs of phase space variables (θ^j, I_j) with all the θ^j cyclic, so that its Hamiltonian depends only on the momenta, $H = H(\vec{I})$. Here, the Kronecker symbol δ^j_k is equal to one for $j = k$ and zero otherwise. It follows that the 'angle' variables θ^j evolve linearly in time ($\theta^j(t) = \theta^j(0) + \omega^j t$) while the momentum or 'action' variables I_j are conserved. Here, $\omega^j = \dot{\theta}^j = \frac{\partial H}{\partial I_j}$ are n constant frequencies. Typically, the angle variables are periodic, so that the θ^j parametrize circles. The common level sets of the action variables $I_j = c_j$ are, therefore, a family of tori that foliate the phase space. Recall that a torus is a Cartesian product of circles. For instance, for one degree of freedom, θ^1 labels points on a circle S^1 while for 2 degrees of freedom, θ^1 and θ^2 label points on a 2-torus $S^1 \times S^1$ which looks like a vada or doughnut. Trajectories remain on a fixed torus determined by the initial conditions. Under a sufficiently small and smooth perturbation $H(\vec{I}) + gH'(\vec{I}, \vec{\theta})$, Andrei Kolmogorov, Vladimir Arnold and Jürgen Moser showed that some of these 'invariant' tori survive provided the frequencies ω^j are sufficiently 'non-resonant' or 'incommensurate' (i.e., their integral linear combinations do not get 'too small').

Simon Newcomb's project of revising all the orbital data in the solar system established the missing 42″ in the 566″ centennial precession of Mercury's perihelion. This played an important role in validating Einstein's general theory of relativity.

George William Hill was motivated by discrepancies in the lunar perigee calculations. His celebrated paper on this topic was published in 1877 while working with Simon Newcomb at the American Ephemeris and Nautical Almanac . He found a new family of periodic orbits in the circular restricted (Sun–Earth–Moon) three-body problem by using a frame rotating with the Sun's angular velocity instead of that of the Moon. The solar perturbation to lunar motion around the Earth results in differential equations with periodic coefficients. He used Fourier series to convert these ODEs to an infinite system of linear algebraic equations and developed a theory of infinite determinants to solve them and obtain a rapidly converging series solution for lunar motion. He also discovered

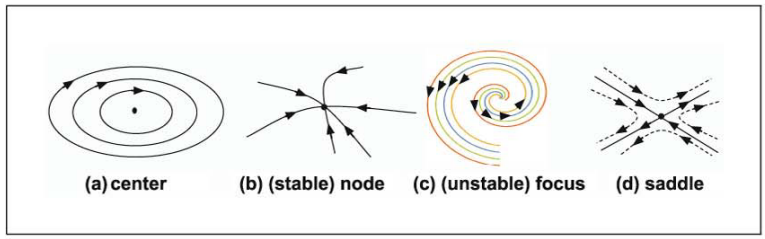

Figure 8. Poincaré's classification of zeros of a vector field (equilibrium or fixed points) on a plane. **(a)** Center is always stable with oscillatory motion nearby, (**b, c**) nodes and foci (or spirals) can be stable or unstable and **(d)** saddles are unstable except in one direction.

new 'tight binary' solutions to the three-body problem where two nearby masses are in nearly circular orbits around their center of mass CM_{12}, while CM_{12} and the far away third mass in turn orbit each other in nearly circular trajectories.

The French mining-engineer/mathematician/physicist Henri Poincaré began by developing a qualitative theory of differential equations from a global geometric viewpoint of the dynamics on phase space. This included a classification of the types of equilibria (zeros of vector fields) on the phase plane (centers, nodes, foci and saddles, see *Figure* 8). His 1890 memoir on the three-body problem was the prize-winning entry in King Oscar II's 60th birthday competition (for a detailed account see [9]). He proved the divergence of series solutions for the three-body problem developed by Delaunay, Hugo Gyldén and Lindstedt (in many cases) and convergence of Hill's infinite determinants. To investigate the stability of three-body motions, Poincaré defined his 'surfaces of section' and a discrete-time dynamics via the 'return map' (see *Figure* 9a). A Poincaré surface S is a two-dimensional surface in phase space transversal to trajectories. The first return map takes a point q_1 on S to q_2, which is the next intersection of the trajectory through q_1 with S. Given a saddle point p on a surface S, he defined its stable and unstable spaces W_s and W_u as points on S that tend to p upon repeated forward or backward applications of the return map (see *Figure* 9b). He initially assumed that W_s and W_u on a surface could not intersect and used this to argue that the solar system is stable. This assumption turned out to be false, as he discovered with the help of Lars Phragmén. In fact, W_s and W_u can intersect transversally on a surface at a homoclinic point if the state space of the underlying continuous dynamics is at least three-dimensional. What is more, he showed that if there is one

Homoclinic refers to the property of being 'inclined' both forward and backward in time to the same point.

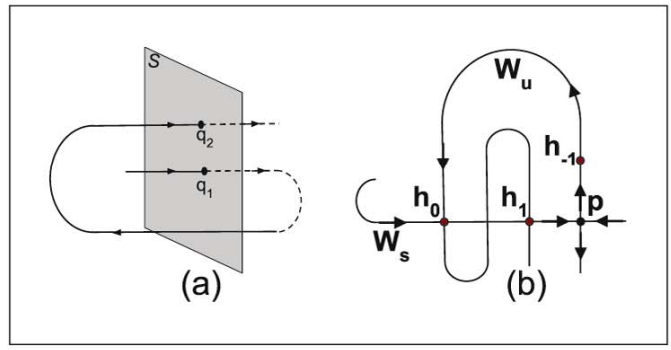

Figure 9. **(a)** A Poincaré surface S transversal to a trajectory is shown. The trajectory through q_1 on S intersects S again at q_2. The map taking q_1 to q_2 is called Poincaré's first return map. **(b)** The saddle point p and its stable and unstable spaces W_s and W_u are shown on a Poincaré surface through p. The points at which W_s and W_u intersect are called homoclinic points, e.g., h_0, h_1 and h_{-1}. Points on W_s (or W_u) remain on W_s (or W_u) under forward and backward iterations of the return map. Thus, the forward and backward images of a homoclinic point under the return map are also homoclinic points. In the figure h_0 is a homoclinic point whose image is h_1 on the segment $[h_0, p]$ of W_s. Thus, W_u must fold back to intersect W_s at h_1. Similarly, if h_{-1} is the backward image of h_0 on W_u, then W_s must fold back to intersect W_u at h_{-1}. Further iterations produce an infinite number of homoclinic points accumulating at p. The first example of a homoclinic tangle was discovered by Poincaré in the restricted three-body problem and is a signature of its chaotic nature.

homoclinic point, then there must be infinitely many accumulating at p. Moreover, W_s and W_u fold and intersect in a very complicated 'homoclinic tangle' in the vicinity of p. This was the first example of what we now call chaos. Chaos is usually manifested via an extreme sensitivity to initial conditions (exponentially diverging trajectories with nearby initial conditions).

When two gravitating point masses collide, their relative speed diverges and solutions to the EOM become singular at the collision time t_c. More generally, a singularity occurs when either a position or velocity diverges in finite time. The Frenchman Paul Painlevé (1895) showed that binary and triple collisions are the only possible singularities in the three-body problem. However, he conjectured that non-collisional singularities (e.g., where the separation between a pair of bodies goes to infinity in finite time) are possible for four or more bodies.

It took nearly a century for this conjecture to be proven, culminating in the work of Donald Saari and Zhihong Xia (1992) and Joseph Gerver (1991) who found explicit examples of non-collisional singularities in the 5-body and $3n$-body problems for n sufficiently large [14]. In Xia's example, a particle oscillates with ever growing frequency and amplitude between two pairs of tight binaries. The separation between the binaries diverges in finite time, as does the velocity of the oscillating particle.

The Italian mathematician Tulio Levi-Civita (1901) attempted to avoid singularities and thereby 'regularize' collisions in the three-body problem by a change of variables in the differential equa-

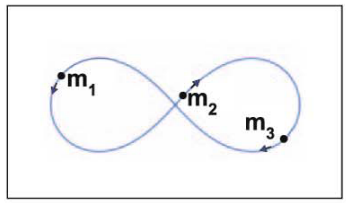

Figure 10. Equal-mass zero-angular momentum figure-8 choreography solution to the three-body problem. A choreography is a periodic solution where all masses traverse the same orbit separated equally in time.

tions. For example, the ODE for the one-dimensional Kepler problem $\ddot{x} = -k/x^2$ is singular at the collision point $x = 0$. This singularity can be regularized by introducing a new coordinate $x = u^2$ and a reparametrized time $ds = dt/u^2$, which satisfy the nonsingular oscillator equation $u''(s) = Eu/2$ with conserved energy $E = (2\dot{u}^2 - k)/u^2$. Such regularizations could shed light on near-collisional trajectories ('near misses') provided the differential equations remain physically valid.

Solutions which could be smoothly extended beyond collision time (e.g., the bodies elastically collide) were called regularizable. Those that could not were said to have an essential or transcendent singularity at the collision.

The Finnish mathematician Karl Sundman (1912) began by showing that binary collisional singularities in the three-body problem could be regularized by a reparametrization of time, $s = |t_1 - t|^{1/3}$ where t_1 is the the binary collision time [15]. He used this to find a *convergent* series representation (in powers of s) of the general solution of the three-body problem in the absence of triple collisions. The possibility of such a convergent series had been anticipated by Karl Weierstrass in proposing the three-body problem for King Oscar's 60th birthday competition. However, Sundman's series converges exceptionally slowly and has not been of much practical or qualitative use.

The point-particle approximation to the equations for celestial bodies of non-zero size breaks down due to tidal effects when the bodies get very close.

The advent of computers in the 20th century allowed numerical investigations into the three-body (and more generally the n-body) problem. Such numerical simulations have made possible the accurate placement of satellites in near-Earth orbits as well as our missions to the Moon, Mars and the outer planets. They have also facilitated theoretical explorations of the three-body problem including chaotic behavior, the possibility for ejection of one body at high velocity (seen in hypervelocity stars [16]) and quite remarkably, the discovery of new periodic solutions. For instance, in 1993, Chris Moore discovered the zero angular momentum figure-8 'choreography' solution. It is a stable peri-

Sundman showed that for non-zero angular momentum, there are no triple collisions in the three-body problem.

odic solution with bodies of equal masses chasing each other on an ∞-shaped trajectory while separated equally in time (see *Figure* 10). Alain Chenciner and Richard Montgomery [17] proved its existence using an elegant geometric reformulation of Newtonian dynamics that relies on the variational principle of Euler and Maupertuis.

8. Geometrization of Mechanics

The optical path length $\int n(\mathbf{r})\, d\tau$ is proportional to $\int d\tau/\lambda$, which is the geometric length in units of the local wavelength $\lambda(\mathbf{r}) = c/n(\mathbf{r})\nu$. Here, c is the speed of light in vacuum and ν the constant frequency.

Fermat's principle in optics states that light rays extremize the optical path length $\int n(\mathbf{r}(\tau))\, d\tau$ where $n(\mathbf{r})$ is the (position dependent) refractive index and τ a parameter along the path. The variational principle of Euler and Maupertuis (1744) is a mechanical analogue of Fermat's principle [18]. It states that the curve that extremizes the abbreviated action $\int_{\mathbf{q}_1}^{\mathbf{q}_2} \mathbf{p} \cdot d\mathbf{q}$ holding energy E and the end-points $\mathbf{q}_1$ and $\mathbf{q}_2$ fixed has the same shape as the Newtonian trajectory. By contrast, Hamilton's principle of extremal action (1835) states that a trajectory going from $\mathbf{q}_1$ at time t_1 to $\mathbf{q}_2$ at time t_2 is a curve that extremizes the action. Here, the action is the integral of the Lagrangian $S = \int_{t_1}^{t_2} L(\mathbf{q}, \dot{\mathbf{q}})\, dt$. Typically, $L = T - V$ is the difference between kinetic and potential energies.

A metric m_{ij} on an n-dimensional configuration space M is an $n \times n$ matrix at each point $\mathbf{q} \in M$ that determines the square of the distance $(ds^2 = \sum_{i,j=1}^{n} m_{ij} dq^i dq^j)$ from $\mathbf{q}$ to a nearby point $\mathbf{q} + d\mathbf{q}$. We often suppress the summation symbol and follow the convention that repeated indices are summed from 1 to n.

It is well-known that the trajectory of a free particle (i.e., subject to no forces) moving on a plane is a straight line. Similarly, trajectories of a free particle moving on the surface of a sphere are great circles. More generally, trajectories of a free particle moving on a curved space (Riemannian manifold M) are geodesics (curves that extremize length). Precisely, for a mechanical system with configuration space M and Lagrangian $L = \frac{1}{2} m_{ij}(\mathbf{q}) \dot{q}^i \dot{q}^j$, Lagrange's equations $\frac{dp_i}{dt} = \frac{\partial L}{\partial q^i}$ are equivalent to the geodesic equations with respect to the 'kinetic metric' m_{ij} on M:

$$m_{ij}\, \ddot{q}^j(t) = -\frac{1}{2} \left(m_{ji,k} + m_{ki,j} - m_{jk,i} \right) \dot{q}^j(t)\, \dot{q}^k(t). \qquad (33)$$

Here, $m_{ij,k} = \partial m_{ij}/\partial q^k$ and $p_i = \frac{\partial L}{\partial \dot{q}^i} = m_{ij}\dot{q}^j$ is the momentum conjugate to coordinate q^i. For instance, the kinetic metric ($m_{rr} = m$, $m_{\theta\theta} = mr^2$, $m_{r\theta} = m_{\theta r} = 0$) for a free particle moving on a

plane may be read off from the Lagrangian $L = \frac{1}{2}m(\dot{r}^2 + r^2\dot{\theta}^2)$ in polar coordinates, and the geodesic equations shown to reduce to Lagrange's equations of motion $\ddot{r} = r\dot{\theta}^2$ and $d(mr^2\dot{\theta})/dt = 0$.

Box 11. Gaussian Curvature

Given a point p on a surface S embedded in three dimensions, a normal plane through p is one that is orthogonal to the tangent plane at p. Each normal plane intersects S along a curve whose best quadratic approximation at p is called its osculating circle. The principal radii of curvature $R_{1,2}$ at p are the maximum and minimum radii of osculating circles through p. The Gaussian curvature $K(p)$ is defined as $1/R_1R_2$ and is taken positive if the centers of the corresponding osculating circles lie on the same side of S and negative otherwise.

Remarkably, the correspondence between trajectories and geodesics continues to hold even in the presence of conservative forces derived from a potential V. Indeed, trajectories of the Lagrangian $L = T - V = \frac{1}{2}m_{ij}(\mathbf{q})\dot{q}^i\dot{q}^j - V(\mathbf{q})$ are *reparametrized*[2] geodesics of the Jacobi–Maupertuis (JM) metric $g_{ij} = (E - V(\mathbf{q}))m_{ij}(\mathbf{q})$ on M where $E = T + V$ is the energy. This geometric formulation of the Euler–Maupertuis principle (due to Jacobi) follows from the observation that the square of the metric line element

[2] The shapes of trajectories and geodesics coincide but the Newtonian time along trajectories is not the same as the arc-length parameter along geodesics.

$$\begin{aligned} ds^2 &= g_{ij}dq^i dq^j = (E-V)m_{ij}dq^i dq^j = \frac{1}{2}m_{kl}\frac{dq^k}{dt}\frac{dq^l}{dt}m_{ij}dq^i dq^j \\ &= \frac{1}{2}\left(m_{ij}\dot{q}^i dq^j\right)^2 = \frac{1}{2}(\mathbf{p}\cdot d\mathbf{q})^2, \end{aligned} \tag{34}$$

so that the extremization of $\int \mathbf{p}\cdot d\mathbf{q}$ is equivalent to the extremization of arc length $\int ds$. Loosely, the potential $V(\mathbf{q})$ on the configuration space plays the role of an inhomogeneous refractive index. Though trajectories and geodesics are the same curves, the Newtonian time t along trajectories is in general different from the arc-length parameter s along geodesics. They are related by $\frac{ds}{dt} = \sqrt{2}(E - V)$ [19].

Loosely, the potential in particle mechanics plays the role of a variable refractive index in optics.

This geometric reformulation of classical dynamics allows us to assign a local curvature to points on the configuration space. For instance, the Gaussian curvature K of a surface at a point (see

Nearby geodesics on a surface of negative curvature diverge exponentially.

Box 11) measures how nearby geodesics behave (see *Figure* 11), they oscillate if $K > 0$ (as on a sphere), diverge exponentially if $K < 0$ (as on a hyperboloid) and linearly separate if $K = 0$ (as on a plane). Thus, the curvature of the Jacobi–Maupertuis metric defined above furnishes information on the stability of trajectories. Negativity of curvature leads to sensitive dependence on initial conditions and can be a source of chaos.

In the planar Kepler problem, the Hamiltonian (5) in the CM frame is

$$H = \frac{p_x^2 + p_y^2}{2m} - \frac{\alpha}{r} \quad \text{where} \quad \alpha = GMm > 0 \ \text{ and } \ r^2 = x^2 + y^2. \tag{35}$$

A compact Riemann surface is a closed, oriented and bounded surface such as a sphere, a torus or the surface of a pretzel. The genus of such a surface is the number of handles: zero for a sphere, one for a torus and two or more for higher handle-bodies. Riemann surfaces with genus two or more admit metrics with constant negative curvature.

The corresponding JM metric line element in polar coordinates is $ds^2 = m\left(E + \frac{\alpha}{r}\right)\left(dr^2 + r^2 d\theta^2\right)$. Its Gaussian curvature $K = -E\alpha/2m(\alpha + Er)^3$ has a sign opposite to that of energy everywhere. This reflects the divergence of nearby hyperbolic orbits and oscillation of nearby elliptical orbits. Despite negativity of curvature and the consequent sensitivity to initial conditions, hyperbolic orbits in the Kepler problem are not chaotic: particles simply fly off to infinity and trajectories are quite regular. On the other hand, negativity of curvature without any scope for escape can lead to chaos. This happens with geodesic motion on a compact Riemann surface with constant negative curvature: most trajectories are very irregular [2].

9. Geometric Approach to the Planar Three-Body Problem

We now sketch how the above geometrical framework may be usefully applied to the three-body problem. The configuration space of the planar three-body problem is the space of triangles on the plane with masses at the vertices. It may be identified with six-dimensional Euclidean space ($\mathbb{R}^6$) with the three planar Jacobi vectors $\mathbf{J}_{1,2,3}$ (see (9) and *Figure* 2) furnishing coordinates on it. A simultaneous translation of the position vectors of all three bodies $\mathbf{r}_{1,2,3} \mapsto \mathbf{r}_{1,2,3} + \mathbf{r}_0$ is a symmetry of the Hamiltonian $H = T + V$ of Eqs. (10, 11) and of the Jacobi–Maupertuis metric

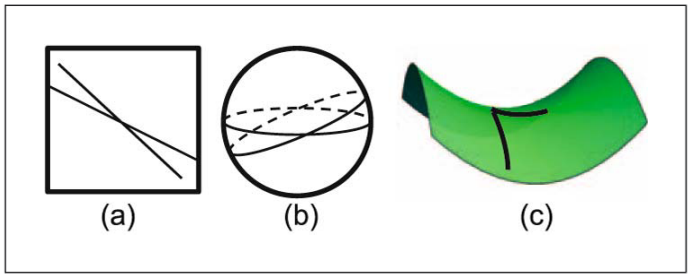

Figure 11. Local behavior of nearby geodesics on a surface depends on the sign of its Gaussian curvature K. **(a)** Nearby geodesics on a plane ($K = 0$) separate linearly. **(b)** Distance between neighbouring geodesics on a sphere ($K > 0$) oscillates. **(c)** Geodesics on a hyperbolic surface ($K < 0$) deviate exponentially.

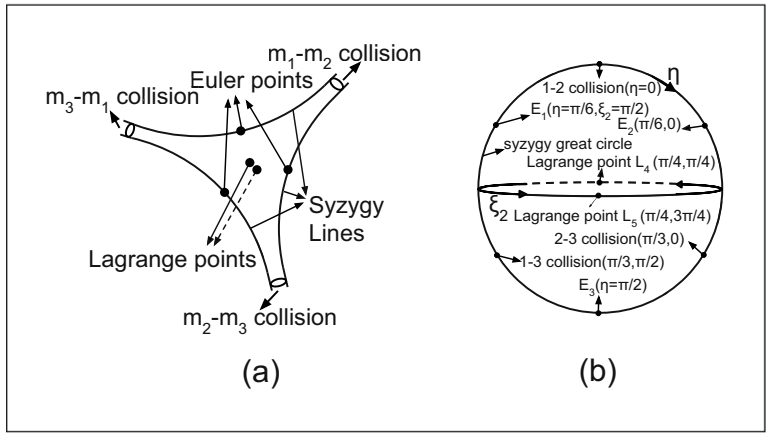

Figure 12. 'Pair of pants' metric on shape sphere and Lagrange, Euler and collision points. **(a)** The negatively curved 'pair of pants' metric on the shape sphere $\mathbb{S}^2$. **(b)** Locations of Lagrange, Euler and collision points on a geometrically *unfaithful* depiction of the shape sphere $\mathbb{S}^2$. The negative curvature of $\mathbb{S}^2$ is indicated in (a). Syzygies are instantaneous configurations where the three bodies are collinear (eclipses).

$$ds^2 = (E - V(\mathbf{J}_1, \mathbf{J}_2)) \sum_{a=1}^{3} M_a \, |d\mathbf{J}_a|^2. \qquad (36)$$

This is encoded in the cyclicity of $\mathbf{J}_3$. Quotienting by translations allows us to define a center of mass configuration space $\mathbb{R}^4$ (the space of centered triangles on the plane with masses at the vertices) with its quotient JM metric. Similarly, rotations $\mathbf{J}_a \rightarrow \begin{pmatrix} \cos\theta & -\sin\theta \\ \sin\theta & \cos\theta \end{pmatrix} \mathbf{J}_a$ for $a = 1, 2, 3$ are a symmetry of the metric, corresponding to rigid rotations of a triangle about a vertical axis through the CM. The quotient of $\mathbb{R}^4$ by such rotations is the *shape space* $\mathbb{R}^3$, which is the space of congruence classes of centered oriented triangles on the plane. Translations and rotations are symmetries of any central inter-particle potential, so the

> Translations and rotations are symmetries of any central inter-particle potential.

dynamics of the three-body problem in any such potential admits a consistent reduction to geodesic dynamics on the shape space $\mathbb{R}^3$. Interestingly, for an *inverse-square* potential (as opposed to the Newtonian '$1/r$' potential)

$$V = -\sum_{a<b} \frac{Gm_a m_b}{|\mathbf{r}_a - \mathbf{r}_b|^2} = -\frac{Gm_1 m_2}{|\mathbf{J}_1|^2} - \frac{Gm_2 m_3}{|\mathbf{J}_2 - \mu_1 \mathbf{J}_1|^2} - \frac{Gm_3 m_1}{|\mathbf{J}_2 + \mu_2 \mathbf{J}_1|^2} \tag{37}$$

with $\mu_{1,2} = m_{1,2}/(m_1 + m_2)$, the zero-energy JM metric (12) is also invariant under the scale transformation $\mathbf{J}_a \to \lambda \mathbf{J}_a$ for $a = 1, 2$ and 3 (see *Box* 12 for more on the inverse-square potential and for why the zero-energy case is particularly interesting). This allows us to further quotient the shape space $\mathbb{R}^3$ by scaling to get the shape sphere $\mathbb{S}^2$, which is the space of similarity classes of centered oriented triangles on the plane[3]. Note that collision configurations are omitted from the configuration space and its quotients. Thus, the shape sphere is topologically a 2-sphere with the three binary collision points removed. In fact, with the JM metric, the shape sphere looks like a 'pair of pants' (see *Figure* 12a).

[3] Though scaling is not a symmetry for the Newtonian gravitational potential, it is still useful to project the motion onto the shape sphere.

Box 12. Inverse Square Potential and its Behavior Under Scaling

The inverse-square potential is somewhat simpler than the Newtonian one due to the behavior of the Hamiltonian $H = \sum_a \mathbf{p}_a^2/2m_a - \sum_{a<b} Gm_a m_b/|\mathbf{r}_a - \mathbf{r}_b|^2$ under scale transformations $\mathbf{r}_a \to \lambda \mathbf{r}_a$ and $\mathbf{p}_a \to \lambda^{-1}\mathbf{p}_a$: $H(\lambda \mathbf{r}, \lambda^{-1}\mathbf{p}) = \lambda^{-2} H(\mathbf{r}, \mathbf{p})$ [6]. The infinitesimal version ($\lambda \approx 1$) of this transformation is generated by the dilatation operator $D = \sum_a \mathbf{r}_a \cdot \mathbf{p}_a$ via Poisson brackets $\{\mathbf{r}_a, D\} = \mathbf{r}_a$ and $\{\mathbf{p}_a, D\} = -\mathbf{p}_a$. Here, the PB between coordinates and momenta are $\{r_{ai}, p_{bj}\} = \delta_{ab}\delta_{ij}$ where a, b label particles and i, j label Cartesian components. In terms of PBs, time evolution of any quantity f is given by $\dot{f} = \{f, H\}$. It follows that $\dot{D} = \{D, H\} = 2H$, so scaling is a symmetry of the Hamiltonian (and D is conserved) only when the energy vanishes. To examine long-time behavior we consider the evolution of the moment of inertia in the CM frame $I_{\mathrm{CM}} = \sum_a m_a \mathbf{r}_a^2$ whose time derivative may be expressed as $\dot{I} = 2D$. This leads to the Lagrange–Jacobi identity $\ddot{I} = \{\dot{I}, H\} = \{2D, H\} = 4E$ or $I = I(0) + \dot{I}(0)\, t + 2E\, t^2$. Hence when $E > 0$, $I \to \infty$ as $t \to \infty$ so that bodies fly apart asymptotically. Similarly, when $E < 0$ they suffer a triple collision. When $E = 0$, the sign of $\dot{I}(0)$ controls asymptotic behavior leaving open the special case when $E = 0$ and $\dot{I}(0) = 0$. By contrast, for the Newtonian potential, the Hamiltonian transforms as $H(\lambda^{-2/3}\mathbf{r}, \lambda^{1/3}\mathbf{p}) = \lambda^{2/3} H(\mathbf{r}, \mathbf{p})$ leading to the Lagrange–Jacobi identity $\ddot{I} = 4E - 2V$. This is however not adequate to determine the long-time behavior of I when $E < 0$.

For equal masses and $E = 0$, the quotient JM metric on the shape

sphere may be put in the form

$$ds^2 = Gm^3 h(\eta, \xi_2)\left(d\eta^2 + \sin^2 2\eta\, d\xi_2^2\right). \qquad (38)$$

Here, $0 \le 2\eta \le \pi$ and $0 \le 2\xi_2 \le 2\pi$ are polar and azimuthal angles on the shape sphere $\mathbb{S}^2$ (see *Figure* 12b). The function h is invariant under the above translations, rotations and scalings and therefore a function on $\mathbb{S}^2$. It may be written as $v_1 + v_2 + v_3$ where $v_1 = I_{\rm CM}/(m|\mathbf{r}_2 - \mathbf{r}_3|^2)$ etc., are proportional to the inter-particle potentials [19]. As shown in *Figure* 12a, the shape sphere has three cylindrical horns that point toward the three collision points which lie at an infinite geodesic distance. Moreover, this equal-mass, zero-energy JM metric (38) has negative Gaussian curvature everywhere except at the Lagrange and collision points where it vanishes. This negativity of curvature implies geodesic instability (nearby geodesics deviate exponentially) as well as the uniqueness of geodesic representatives in each 'free' homotopy class, when they exist. The latter property was used by Montgomery [17] to establish uniqueness of the 'figure-8' solution (upto translation, rotation and scaling) for the inverse-square potential. The negativity of curvature on the shape sphere for equal masses extends to negativity of scalar curvature on the CM configuration space for both the inverse-square and Newtonian gravitational potentials [19]. This could help to explain instabilities and chaos in the three-body problem.

The shape sphere is negatively curved at all points other than Lagrange and collision points. It has three horns that point towards the collision points which lie at an infinite distance.

Scalar curvature is an average of the Gaussian curvatures in the various tangent planes through a point

Acknowledgement

We thank A Thyagaraja for useful comments. This work was supported in part by the Infosys Foundation.

Suggested Reading

[1] J Laskar, Is the Solar System Stable?, *Progress in Mathematical Physics*, Vol.66, pp.239–270, 2013.

[2] M C Gutzwiller, *Chaos in Classical and Quantum mechanics*, Springer-Verlag, New York, 1990.

[3] S Bodenmann, The 18th-century Battle Over Lunar Motion, *Physics Today*, Vol.63, No.1, p.27, 2010.

[4] H Goldstein, C P Poole and J L Safko, *Classical Mechanics*, 3rd Ed., Pearson Education, 2011.

[5] L N Hand and J D Finch, *Analytical Mechanics*, Cambridge Univ. Press, 1998.

[6] S G Rajeev, *Advanced Mechanics: From Euler's Determinism to Arnold's Chaos*, Oxford University Press, Oxford, 2013.

[7] F Diacu and P Holmes, *Celestial Encounters: The Origins of Chaos and Stability*, Princeton University Press, New Jersey, 1996.

[8] Z E Musielak and B Quarles, The Three-body Problem, *Reports on Progress in Physics*, Vol.77, No.6, p.065901, 2014, arXiv:1508.02312.

[9] J Barrow-Green, Poincaré and the Three Body Problem, *Amer. Math. Soc.*, Providence, Rhode Island, 1997.

[10] E T Whittaker, *A Treatise on the Analytical Dynamics of Particles & Rigid Bodies*, 2nd Ed., Cambridge University Press, Cambridge, 1917, Chapt. XIV and p.283.

[11] K R Symon, *Mechanics*, 3rd Ed., Addison Wesley, Philippines 1971.

[12] N Mukunda, Sir William Rowan Hamilton, *Resonance*, 21, No.6, p.493, 2016.

[13] M C Gutzwiller, Moon-Earth-Sun: The Oldest Three-body Problem, *Reviews of Modern Physics*, Vol.70, p.589, 1998.

[14] D G Saari and Z Xia, Off to Infinity in Finite Time, *Notices of the AMS*, Vol.42, p.538, 1993,

[15] C L Siegel and J K Moser, *Lectures on Celestial Mechanics*, Springer-Verlag, Berlin, p.31, 1971.

[16] W R Brown, Hypervelocity Stars in the Milky Way, *Physics Today*, Vol.69, No.6, p.52, 2016.

[17] R Montgomery, A New Solution to the Three-body Problem, *Notices of the AMS*, Vol.48, No.5, p.471, 2001.

[18] C Lanczos, *The Variational Principles of Mechanics*, 4th Ed., Dover, New York, p.139, 1970.

[19] G S Krishnaswami and H Senapati, Curvature and Geodesic Instabilities in a Geometrical Approach to the Planar Three-body Problem, *J. Math. Phys.*, Vol.57, p.102901, 2016, arXiv:1606.05091.

Address for Correspondence
Govind S Krishnaswami[1]
Himalaya Senapati[2]
Chennai Mathematical Institute
SIPCOT IT Park
Siruseri 603 103
India.
Email: govind@cmi.ac.in[1]
himalay@cmi.ac.in[2]